STRUCTURAL DYNAMICS RESEARCH IN A FULL-SCALE TRANSPORT AIRCRAFT CRASH TEST

Harvey G. McComb, Jr.; Robert G. Thomson*; and Robert J. Hayduk
NASA Langley Research Center
Hampton, Virginia 23665-5225

ICAS-86-4.5.1

Abstract

A remotely piloted air-to-ground crash test of a full-scale transport aircraft was conducted for the first time for two purposes: (1) to demonstrate performance of an anti-misting fuel additive in suppressing fire in a crash environment, and (2) to obtain structural dynamics data under crash conditions for comparison with analytical predictions. The test, called the Controlled Impact Demonstration (CID), was sponsored by the Federal Aviation Administration (FAA) and the National Aeronautics and Space Administration (NASA) with cooperation of industry, the Department of Defense, and the British and French governments. The test aircraft was a Boeing 720 jet transport. The aircraft impacted a dry lakebed at Edwards Air Force Base, California. The primary interest of the FAA in this experiment was demonstration of performance of anti-misting fuel additive. The primary interest of NASA was collection of structural crash dynamics data and correlation with analysis.

Prior to the CID, drop tests were conducted on fuselage sections representative of the B-720 aircraft. These tests aided in the development of data acquisition equipment to measure crash loads in the structure and mathematical models to calculate the structural crash behavior. The purpose of this paper is to discuss the structural aspects of the CID. The fuselage section tests and the CID itself are described. Structural response data from these tests are presented and discussed. Nonlinear analytical modeling efforts are described, and comparisons between analytical results and experimental results are presented.

I. Introduction

Full-scale crash tests have been conducted in the United States for over 35 years to help understand how aircraft structures behave in crash situations. Of particular interest are causes of passenger injury and fatalities resulting from severe, but potentially survivable crashes. In the 1950's the National Advisory Committee for Aeronautics conducted crash tests on light aircraft, fighters, and transports[1,2]. In the 1960's the Federal Aviation Administration (FAA) conducted tests on a DC-7 and a Lockheed Constellation[3,4]. From 1972 to 1983 the National Aeronautics and Space Administration (NASA) conducted over 30 crash tests on general aviation aircraft and helicopters[5]. All of these experiments were ground based--either ground-to-ground runs into barriers or swing tests from a gantry into the ground. On December 1, 1984, the FAA and NASA conducted the first remotely piloted air-to-ground full-scale crash test of a transport aircraft. The aircraft, a Boeing 720 jet-powered transport, was remotely piloted to an impact point on the desert at Edwards Air Force Base, California. The test, called a Full-Scale Transport Controlled Impact Demonstration (CID), culminated four years of effort by the two agencies with the cooperation of industry, Department of Defense, and the British and French Governments[6]. The primary objectives of this experiment were: (1) to demonstrate a fuel additive called anti-misting kerosene (AMK) intended to suppress crash-related fires, and (2) to gather crash dynamics data on airframe structure, seats and anthropomorphic dummies, and selected equipment.

Program management, the AMK experiment, equipment experiments, and most of the seat and dummy experiments were the responsibility of the FAA. Acquisition of airframe structural response data, subsequent analysis of this data, and development and validation of an airframe mathematical structural model using the computer program DYCAST were the responsibility of NASA Langley Research Center (LaRC). Selection, testing and installation of instrumentation for measuring the impact loads throughout the aircraft structure and into seats, dummies and equipment were also the responsibility of LaRC. Two independent 176-channel Data Acquisition Systems (DAS) for recording and transmitting crash loads data and a 10-camera photographic system for on-board high-speed film coverage were developed, tested, and qualified by LaRC. As part of the preparation for CID, the development of data acquisition equipment, and the development of mathematical structural models, preliminary tests were conducted by both LaRC and FAA on full-scale fuselage sections.

The remote control system and supporting simulator and a developmental manned flight program in preparation for remotely piloting the test aircraft to the impact site were the responsibility of NASA Ames Dryden Flight Research Center (DFRF), located at Edwards Air Force Base. A telemetry system for ground-based control of the aircraft and for recording the telemetered experimental data was developed by DFRF. Systems integration was also the responsibility of DFRF, that is, they integrated the FAA AMK and equipment experiments, LaRC structural measurement experiments, on-board photographic system, data acquisition and transmission equipment, and all associated electronics.

The purpose of this paper is to discuss structural response data from the CID and from fuselage section drop tests conducted before the CID. In addition, nonlinear analytical modeling efforts to predict both the global airframe structural behavior in the CID and the fuselage section behavior in the section tests are discussed.

II. Fuselage Section Tests

The goal of the research discussed in this paper was comparison of test and analysis results from the transport aircraft shown in Figure 1. To help understand transport fuselage behavior under crash conditions, aid in development of mathematical models of the aircraft structure, and aid in development of data acquisition equipment, preliminary tests were conducted on fuselage sections. Three such tests were conducted at LaRC

*Deceased, formerly Head, Impact Dynamics Branch

on 3.7 m (12 ft) long sections of fuselage representing locations shown in Figure 2. The forward and aft sections are completely clear of the wing. The center section includes the aft wing-box carry-through spar and keel beam and wheel wells. The forward section is shown ready for test in Figure 3. These fuselage test articles were actually from Boeing 707 aircraft, which have basically the same fuselage cross-section as the Boeing 720. In addition to these tests, the FAA conducted a B-707 section drop test and a DC-10 wide-body jet transport fuselage section drop test.

The fuselage sections tested at LaRC were loaded with seats, anthropomorphic dummies, and instrumentation, but interior paneling, insulation, storage bins, and ducting had been removed. In each test on the forward and center sections eight 50th percentile (74.8 kg (165 lbm)) anthropomorphic dummies and one 95th percentile (88.5 kg (195 lbm)) anthropomorphic dummy were distributed among four or five triple seats[7,8]. Typically, ballast masses were used to load remaining seat locations. In the aft fuselage section test only one set of seats was installed--a triple seat with three 50th percentile dummies. The remainder of the loading on that section consisted of a DAS pallet and power pallets which were undergoing tests to certify the equipment for the CID. The tests were performed in a vertical test apparatus which provided a stable guide mechanism for the impact. In each test the impact attitude was 0-degree pitch, yaw, and roll, and the impact velocity was 6.1 m/s (20 ft/s). The sections were dropped a little over 1.8 m (6 ft) and impacted on a concrete pad.

III. CID Test Aircraft

The aircraft used in this demonstration was a Boeing 720, four-engine, intermediate range, jet transport purchased new by the FAA in October 1960. The aircraft was used for flight training of operations inspectors. Even though the Boeing 720 is an old aircraft, its structural design and construction are still representative of narrow-body jet transport aircraft currently in airline service.

Modifications were made to the aircraft for the AMK experiment[9]. The fuel delivery system was extensively modified, and each engine carried a turbine-driven AMK-fuel degrader device to change the properties of the AMK so that the fuel characteristics were nearly those of Jet A fuel prior to entering the engine.

The floor plan of the CID aircraft is presented in Figure 4 and shows location of seats and DAS pallets. Other hardware in the aircraft consisted of four power pallets for cameras and lights, ten cameras, and associated lights. A total of 350 instruments were located throughout the fuselage structure, wings, storage bins, seats and dummies as listed in Table 1. The distribution was 45 percent on seats and dummies and 55 percent on structure. The vast majority of transducers were accelerometers (305). The remaining 45 channels were strain gage type transducers.

Instrumentation layout of the aircraft is shown in Figure 5. Basically, seven major frames distributed along the length of the fuselage were instrumented from belly to crown with accelerometers to measure load transmission during the impact (Fig. 5a). The cross-sectional views show the distribution of instrumentation at a particular frame. Eight strain gage bending bridges were installed near these major frames to measure fuselage bending moment during impact. Wing instrumentation (Fig. 5b) was limited and primarily intended to measure vertical loads transmitted along the spars. Both inboard pylons had two accelerometers at the engine connections (Fig. 5c). These transducers measure the load transmission from engines to the wings.

IV. CID Impact Scenario

The impact scenario for the CID was selected after detailed studies of 176 well-documented survivable jet transport accidents which occurred between 1958 and 1979[10,11]. The planned scenario is illustrated in Figure 6. The aircraft would follow a 3.3 to 4.0 degree glide slope in a 1.0 degree nose-up attitude with landing gear retracted. The aircraft would have a nominal sink rate of 5.2 m/s (17 ft/s) with no roll or yaw, a longitudinal velocity of 269-278 km/hr (167-173 miles/hr or 145-150 knots) and an aircraft gross mass of 79,400-88,500 kg (175,000-195,000 lbm). The planned impact, then, was to be symmetric for crash dynamics measurements followed by a slide through wing openers and obstructions required for the AMK experiment. The intent was for the crash impact to be large enough to cause significant damage to the fuselage, but not so great as to cause complete fuselage break-up.

V. Mathematical Modeling

Mathematical models for structural analysis were developed for the fuselage section test articles and the complete B-720 CID test article using two computer programs--KRASH[12] and DYCAST[13]. The program KRASH was originally developed by Lockheed California Company sponsored by the United States Army and FAA. The program DYCAST was developed by Grumman Aerospace Corporation sponsored by NASA and FAA. DYCAST modeling is reviewed in the present paper.

DYCAST Computer Program

DYCAST is a nonlinear finite element structural analysis computer program with dynamic capabilities. The basic element library consists of: (1) stringers with axial stiffness only; (2) nonlinear springs with user-specified force-displacement relations and hysteresis; (3) beams with axial, two shear, torsional and two bending stiffnesses; (4) isotropic and orthotropic membrane skin triangles with in-plane normal and shear stiffnesses; and (5) isotropic plate bending triangles with membrane and out-of-plane bending stiffnesses.

The nonlinear spring element can be used as an elastic element, a dissipative element, or a gap element such as a ground-contact spring. The changing stiffness in the structure is accounted for by plasticity (material nonlinearity) and large displacements (geometric nonlinearity). Material nonlinearities are accommodated by one of three options: (1) elastic-perfectly-plastic, (2) elastic-linear-hardening-plastic, or (3) elastic-nonlinear-hardening-plastic of the Ramberg-Osgood type. The second option (elastic-linear-hardening-plastic) was used exclusively for this modeling effort. Geometric nonlinearities are handled in an updated Lagrangian formulation by

reforming the structure into its deformed shape after small time increments while accumulating deformations, strains, and forces. The nonlinearities due to combined loadings (such as beam-column effects) are maintained, and stiffness changes due to structural failures are computed. The failure option is imposed automatically whenever a material failure strain criterion is met, or manually by the user at the restart of a simulation.

Numerical time integrators available are two explicit types--fixed-step central difference and modified Adams, and two implicit types--Newmark-beta and Wilson-theta. The latter three have a variable time step capability which is controlled internally by a solution convergence error measure. Thus, the size of the time step is increased and decreased as required during the calculation. The Newmark-beta implicit time integrator was used exclusively for the calculations presented in this paper.

Descriptions of Models

Nonlinear dynamic calculations are very demanding of computer resources with current equipment. Careful attention, therefore, must be focussed on keeping the size and complexity of mathematical models under control. Boeing Commercial Airplane Company made major contributions to this modeling effort under contract to LaRC.

Fuselage Sections. Several different mathematical models were developed for the fuselage sections with graduated degrees of refinement. Models of the forward section only are discussed here. Initially, a single frame model was developed which included substantial detail of frame cross-sections from crown to keel. Based on studies of this model, simplifications were identified which allowed reduction in the number of elements required to model a frame. Subsequently, a two-frame model was developed. This model contained sufficient detail to include the floor, two triple seats with lumped-mass occupants, and the basic fuselage structure without the need for nonlinear springs to represent structure. The two-frame model is shown schematically in Figure 7. Beam elements with appropriate cross-section shapes were used to model the frames below the floor, the floor itself, and seat rails. Less detail was used in modeling the upper fuselage, since this structure was not expected to experience plastic deformations. Four lumped masses connected by horizontal stringers and supported by four nonlinear springs represented the triple seats and occupants. Experimental force-deflection data were used for the seat legs. Because of asymmetry in the seat pan loadings the occupant mass was distributed two-to-one over the inboard and outboard legs, respectively.

The structure was assumed to be symmetric about the fuselage center-line, and computations were performed using a half-model. This half-model consisted of:

Degrees of Freedom	105
Beams	32
Stringers	4
Lumped Masses	16
Ground Springs	6
Seat Springs	4

Nonlinear material properties for the subfloor aluminum frames (beam elements) were elastic-plastic with linear strain hardening.

CID Aircraft. A DYCAST model of the CID Boeing 720 aircraft was also developed. This model represents an aircraft 40 m (131 ft) long and 39 m (128 ft) in wingspan. Detailed modeling for this complete aircraft in the mode used for the fuselage section models would require an excessive number of elements and degrees of freedom. The CID model, therefore, was developed using single and compound beam elements along with nonlinear springs. Schematic sketches of the model are shown in Figures 8 and 9.

The fuselage is modeled with a compound beam representing the cross-sectional properties of the skin-stringer-frame structure of the fuselage. The compound beam is formed by the combination of various beams representing segments of the fuselage constrained to bend as a unit. The moments of inertia of the various beams are maintained at the proper vertical cross-section location in the fuselage. The elements shown in Figure 9 underneath the compound beam which represents the fuselage are nonlinear springs. They represent fuselage crushing, and their properties are estimated from analyses of the fuselage sections and results from fuselage drop tests.

Primary wing structure was modeled as a compound box beam. Engine and pylon structures were modeled as combinations of simple beams. In addition to the modeling indicated in the schematic drawings in Figures 8 and 9, ground springs were included to represent the behavior of the impacted surface.

The planned impact scenario was to be symmetric ground impact--zero roll and zero yaw. Only one half of the aircraft was modeled, therefore. This model of half the aircraft consisted of:

Degrees of Freedom	196
Beams (single and compound)	126
Concentrated Masses	113
Structural Crush Springs	73
Ground Springs	15

External forces applied to the model were gravity, friction (using coefficient of friction of 0.4), and time dependent lift.

VI. Data Filtering

Both experimental and analytical results include a large high-frequency content which can mask the basic crash pulse information being sought. These high frequencies can be attributed to structural vibrations which do not cause structural damage or trauma in occupants. Selection of proper filters to identify crash pulses which can potentially damage structure and cause trauma in occupants was the subject of extensive trials during the early part of the general aviation aircraft crash dynamics research conducted at LaRC from 1972 to 1983. Based on this experience all data presented in this paper (both experimental and analytical) were appropriately filtered[14]. For example, for dummy pelvis locations a 180 Hertz low-pass filter was used, and for structural locations a 100 Hertz low-pass filter was used.

VII. Results and Discussion

Fuselage Sections

Drop Tests. Results from drop tests of the forward and center fuselage sections are published[7,8] Results from drop test of the aft fuselage section are not yet published. A

photograph of the forward fuselage drop test article after test is shown in Figure 10. Gross structural damage was confined to the lower fuselage. All seven frames of the fuselage section ruptured near the bottom contact point. Plastic hinges formed in each frame along both sides of the fuselage. The total post-test crushing distance varied from 0.56-0.58 m (22-23 in.) at the forward end (body station 600) to 0.46-0.48 m (18-19 in.) at the aft end (body station 600J). Motion picture analysis of the forward frame at body station 600 indicated a maximum deflection of approximately 0.66 m (26 in.) occurred 0.21 s after impact. Maximum vertical pelvis accelerations in the dummies in the forward section were 6 to 8 G (180 Hz filter).

Behavior of the aft fuselage section in the drop test was similar to that of the forward section except with higher accelerations. Again, in the aft section test, the gross structural damage was confined to the lower fuselage, and frame rupturing and plastic hinging actions were similar to the forward section results. Maximum vertical pelvis accelerations in the dummies for the aft section test were 9 to 19 G (180 Hz filter).

The center section drop test results were startlingly different, however. The center section is an extremely stiff structure because it contains a sturdy keel structure which separates the main landing gear wheel wells. This center section deformed very little in the drop test. High dynamic loads were transmitted directly from the lower fuselage into the floor, upper fuselage, seats and anthropomorphic dummies. Limited failures occurred in seat structure. Maximum vertical pelvis accelerations were in the range of 40 to 60 G (180 Hz filter) in sharp contrast to results from the other two section tests.

Comparisons Between Test and Analysis. Results are discussed from the forward fuselage section only. Analytical results from the DYCAST mathematical model for the deformed shape are indicated in Figure 11. Values of 345 MPa (50 ksi) yield stress and 0.08 rupture strain were selected empirically to match roughly the overall experimental deformation behavior with the simple linear-strain-hardening plasticity option and the finite element model used for these calculations. These values were used in all calculations for the fuselage section reported in this paper. Comparison between experimental and calculated vertical floor displacements as a function of time at body station 600 is shown in Figure 12. Results for vertical accelerations as a function of time at the joint between the fuselage wall and the floor at body station 600 are shown in Figure 13. Typical results for vertical accelerations at the pelvis of one of the anthropomorphic dummies are shown in Figure 14. Positive vertical acceleration is up. The experimental vertical acceleration histories show two distinct peaks. The first peak corresponds to the acceleration at initial contact. When the frames rupture at the bottom, the load is relieved, and the acceleration decreases. The second peak occurs at the time the frame plastic hinge points impact the concrete surface.

The type of data presented in Figure 12, for example, was used to model crush springs in the CID aircraft mathematical model. These comparisons in Figures 12-14 do not display precise correlations between calculated and experimental results; however, the general trends are predicted, and maximum values of displacements and accelerations correlate reasonably well. Calculations for these plots were made with a constant time increment of 0.000250 s. Computer resources required for this model are indicated by the following data: to run 901 constant time increments (0.225 s real time) required 1620 s (central-processing-unit) on a Control Data Cyber 175 computer with a maximum field memory length of 303K.

CID Flight

Flight Test. At 9:13 a.m. Pacific Standard Time on December 1, 1984, the CID aircraft took off from Edwards Air Force Base, California, for its remotely piloted final flight. Weather conditions were ideal--visibility excellent and wind speed less than 5 knots. The aircraft was under ground-based control of an experienced NASA test pilot. The aircraft climbed to 700 m (2,300 ft) above ground and circled the dry lake bed to intercept a simulated instrument landing system to begin its descent to the impact point. The instrument landing system and a video camera in the nose of the aircraft provided visual cues to aid the pilot.

At an altitude of 61 m (200 ft) the aircraft was off the target centerline, but not enough for the pilot to call a go-around. The 46 m (150 ft) altitude was the agreed-upon commit altitude because of activation of time-critical, limited duration, onboard photographic and data acquisition equipment. At the 46 m (150 ft) altitude the pilot made a left aileron control input to bring the aircraft back to the target centerline. The control input initiated lateral oscillations after commitment, but prior to impact. The pilot concentrated his efforts on damping the oscillations, achieving the best line up possible with the target centerline, and meeting a critical project requirement of impacting the ground in front of the wing openers. The structural and seat experiments were planned for an impact and slide-out prior to contacting the wing opener obstructions for the AMK experiment. Impacting beyond the wing openers would have jeopardized the AMK experiment if fuel spillage had not occurred.

Analysis of motion picture film showed the actual CID crash scenario. A sequence of photographs illustrating the impact is in Figure 15. The left outboard engine nacelle impacted the ground first at 9:22:11 a.m. The aircraft was rolled 13 degrees to the left, yawed 13 degrees to the left, and at zero pitch. The aircraft was traveling at a speed of 278 km/hr (173 miles/hr or 150 knots) with a sink rate of 5.27 m/s (17.3 ft/s) and an estimated gross mass of 87,090 kg (192,000 lbm). The initial impact occurred 125 m (410 ft) short of the planned impact point. After the left nacelles and wing impacted the ground, the aircraft continued to increase left yaw, and the fuselage pitched slightly nose down. The history of aircraft pitch angle for one second starting at initial impact is shown in Figure 16. Approximately 0.46 s after the initial impact and 86.9 m (285 ft) short of the planned impact point, the fuselage struck the ground at a pitch of -2.5 degrees and a center-of-gravity sink rate of 3.66 m/s (12.0 ft/s). The wing, therefore, absorbed kinetic energy and reduced the severity of the fuselage impact. The aircraft yaw gradually increased to 38 degrees left, and the first wing opener was contacted. This wing opener was third from the center-line among the four devices on the right-hand side of the aircraft. It cut through

the right inboard nacelle and engine and diagonally slashed the leading edge and lower wing. The right wing failed, lifted upward as the aircraft continued to slide, and separated from the aircraft, dumping fuel during the process (Fig. 15d). All four wing openers on the right side cut open the fuselage which permitted fuel to enter the fuselage from the bottom. Because of the left yaw condition of the aircraft, none of the four wing openers on the left side of the aircraft struck the aircraft. At 9:22:21 a.m. the aircraft came to rest at a location about 290 m (950 ft) beyond the planned impact point. Results from the AMK experiment on CID are in the publication process[15,16].

Comparisons Between Test and Analysis. In April 1985 a workshop was held in Hampton, Virginia, to discuss all aspects of the crash dynamics experiments on the CID. Proceedings of that workshop containing a limited amount of structural dynamics data have been published[14]. A complete compilation of structural dynamics data in the form of acceleration and bending moment traces for one second of time after initial left wing impact and prior to wing cutter impact has been published[17]. Calculations were made with the symmetric DYCAST model discussed previously. Further calculations are currently in progress for a full airplane DYCAST model simulating the unsymmetric crash scenario which actually occurred, but results are not yet available.

Selected results from the symmetric calculations are presented here and compared with the corresponding test data[17]. The calculation began at the instant the fuselage contacted the ground and continued for 0.15 s. Initial conditions used in the analysis were established from analysis of the film coverage as follows: 273 km/hr (169 miles/hr or 147 knots) horizontal velocity and 3.66 m/s (12.0 ft/s) vertical velocity at the center-of-gravity, pitch of -2.5 degrees, and pitch rate of -0.1 radians per second. To introduce pitch rate into the DYCAST model, the initial velocity of each finite element joint was computed using the velocity vector of the center-of-gravity, the rotational velocity vector about the center-of-gravity, and the radius vector from the center-of-gravity to the joint. Yaw and roll conditions were ignored for this analysis. A side view of the model at time of initial fuselage contact is shown in Figure 17.

Comparisons of experimental and analytical vertical floor accelerations are presented in Figures 18-21 for selected fuselage stations starting at the pilot's location and progressing aft. Positive vertical acceleration is up. The solid lines are experimental data, and the dashed lines are analytical data. The general oscillatory behavior in the experimental data is predicted fairly well by the analysis, although the results are somewhat out of phase. The maximum values or peaks of the acceleration traces and the total 0.15 s crash pulse duration correlate reasonably well.

Comparisons of peak vertical and longitudinal floor accelerations are plotted as a function of distance along fuselage in Figures 22-23. Positive vertical acceleration is up, positive longitudinal acceleration is aft. The square symbols are experimental data, and the circle symbols are analytical data. The analytical results display the same trends as the experimental results, and fairly well represent acceleration peaks for the length of the aircraft fuselage. Calculations for these plots were made with a constant time increment of 0.000500 s which was conservative for this problem. Just to give an idea of computer resources required for this work, to run 300 constant time increments (0.150 s real time) required 1643 s (central-processing-unit) on a Control Data Cyber 175 computer with a maximum field memory length of 337K.

During the post-test inspection of the CID aircraft, measurements were made of the total fuselage crush at selected locations. Because the wing openers ripped out the center section keel beam and the post crash fire destroyed a large portion of the aft fuselage, measurements of crush aft of the wing are not representative of initial impact damage. A comparison of measured and calculated fuselage crush for two locations forward of the wing is shown in Figure 24. The excellent correlation apparent in Figure 24 is perhaps expected since empirical/analytical data from fuselage drop tests were used to describe the crush springs in the mathematical model for the airframe structure.

These comparisons between experimental and analytical accelerations are perhaps not as good as those for the fuselage sections. Nevertheless, the trends are fairly well predicted, and maximum values of accelerations correlate reasonably well. The mathematical models used in this work are not as refined as what is commonly used today to perform linear static stress analysis of transport aircraft structures. A building-block approach was used in which results from detailed models of structural components formed input to larger models leading finally to a full-airplane airframe model. The comparisons achieved with these analytical models and the experimental data indicate the validity of the basic strategy. It is felt, therefore, that the analytical approach typified in this paper can contribute substantially to understanding transport aircraft behavior under crash conditions.

VIII. Summary Remarks

A full-scale remotely piloted air-to-ground crash test was conducted on a Boeing 720 jet transport aircraft, and drop tests were conducted on three fuselage sections representative of this aircraft. A large amount of structural dynamics data was obtained from these tests. The data is published elsewhere in the form of acceleration and bending moment traces as a function of time for use by aircraft engineers in the design of improved aircraft. Finite element mathematical models were developed for structural analysis of these test articles, and comparisons are made between experimental and analytical accelerations. The mathematical models are not as refined as current state-of-the-art models for linear static stress analysis of transport aircraft and involve empirical/analytical input to represent crushing behavior of structure. Nevertheless, correlation among experimental and analytical accelerations both in the fuselage section tests and in the complete aircraft test are reasonably good. The analysis predicts trends and maximum values of local accelerations fairly well. These analyses are very demanding of current computer resources because of their dynamic nature. Future developments in analysis and computer technology will reduce the empiricism required for this type of

calculation. It is believed, however, that the level of analysis represented by the work reported here will continue to serve the engineering community to improve understanding of crash dynamics phenomena.

References

1. Preston, G. Merritt and Pesman, Gerard J.: Accelerations in Transport-Airplane Crashes. NACA TN 4158, 1958.

2. Acker, Loren W.; Black, Dugald O.; and Moser, Jacob C.: Accelerations in Fighter Airplane Crashes. NACA RM E57G11, 1957.

3. Reed, W. H.; Robertson, S. H.; Weinberg, L. W. T.; and Tyndall, L. H.: Full-Scale Dynamic Crash Test of a Douglas DC-7 Aircraft. FAA-ADS-37, April 1965.

4. Reed, W. H.; Robertson, S. H.; Weinberg, L. W. T. ; and Tyndall, L. H.: Full-Scale Dynamic Crash Test of a Lockheed Constellation Model 1649 Aircraft. FAA-ADS-38, October 1965.

5. Thomson, Robert. G.; Carden, Huey D.; and Hayduk, Robert. J.: Survey of NASA Research on Crash Dynamics. NASA TP 2298, April 1984.

6. Blake, Neal A.: Controlled Impact Demonstration Review. SAE Technical Paper 851884. Presented at Society of Automotive Engineers Aerospace Technology Conference and Exposition, Long Beach, California, October 14-17, 1985.

7. Williams, M. Susan; and Hayduk, Robert J.: Vertical Drop Test of a Transport Fuselage Section Located Forward of the Wing. NASA TM 85679, August 1983.

8. Williams, M. Susan; and Hayduk, Robert J.: Vertical Drop Test of a Transport Fuselage Center Section Including the Wheel Wells. NASA TM 85706, October 1983.

9. Anonymous: Full-Scale Transport Controlled Impact Demonstration Program, Management Plan. DOT/FAA/CT-82/151, FAA Technical Center, Atlantic City Airport, New Jersey, January 1984.

10. Hayduk, Robert J.; Alfaro-Bou, Emilio; and Fasanella, Edwin L.: NASA Experiments Onboard the Controlled Impact Demonstration. SAE Technical Paper 851885. Presented at Society of Automotive Engineers Aerospace Technology Conference and Exposition, Long Beach, California, October 14-17, 1985.

11. Thomson, Robert G.; and Caiafa, C.: Structural Response of Transport Airplanes in Crash Situations. NASA TM 85654, June 1983.

12. Soltis, Stephen; Caiafa, Caesar; and Wittlin, Gil: FAA Structural Crash Dynamics Program Update--Transport Category Aircraft. SAE Technical Paper 851887. Presented at Society of Automotive Engineers Aerospace Technology Conference and Exposition, Long Beach, California, October 14-17, 1985.

13. Fasanella, Edwin L.; Widmayer, E.; and Robinson, Martha P.: Structural Analysis of the Controlled Impact Demonstration of a Jet Transport Airplane. Presented at AIAA 27th Structures, Structural Dynamics and Materials Conference, San Antonio, Texas, May 19-21, 1986.

14. Hayduk, Robert J., Compiler: Full-Scale Transport Controlled Impact Demonstration. NASA Conference Publication 2395, 1986.

15. Fenton, Bruce C.: Antimisting Fuel Technology Application in Full-Scale Transport Aircraft. DOT/FAA/CT-TN85/65. To be published.

16. Yaffee, M. L.: Antimisting Fuel Research and Development for Commercial Aircraft. DOT/FAA/CT-86-7. To be published.

17. Fasanella, Edwin L.; Alfaro-Bou, Emilio; and Hayduk, Robert J.: Impact Data From the Controlled Impact Demonstration of a Transport Aircraft. NASA TP 2589, 1986.

Table 1.--CID Instrumentation Summary

Accelerometers

Dummies	52
Seats	75
Structure	178
Overhead Bins	3
Wing Pylons	4
Wing Other	14
Floor Near Seats	43
Frames	109
CG	3
Tail	2
Total	305

Bending Bridges

Wing	4
Fuselage	8
Total	12

Load Cells

Overhead Storage Bins	3
Lap Belt	26
Shoulder Harness	4
Total	33

Grand Total Channels	350

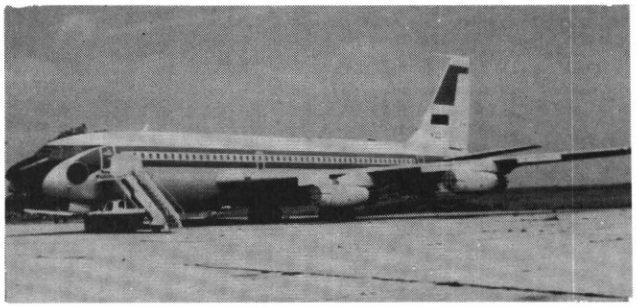

Figure 1. Boeing 720 CID Aircraft

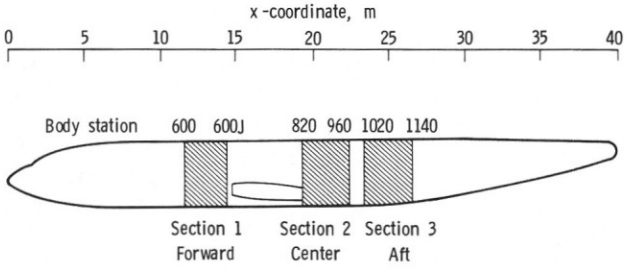

Figure 2. Schematic of Boeing 720 Transport Showing Representative Locations of Fuselage Drop Test Sections

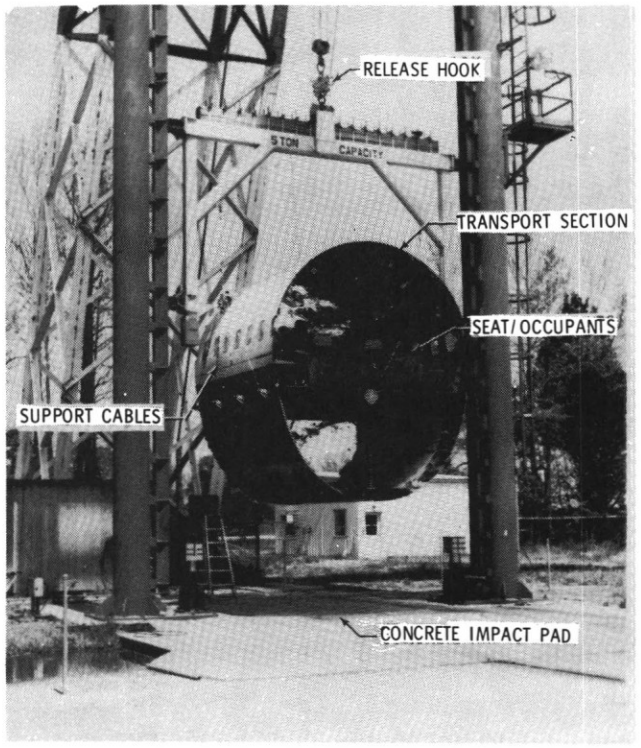

Figure 3. Forward Fuselage Section Prior to Drop Test

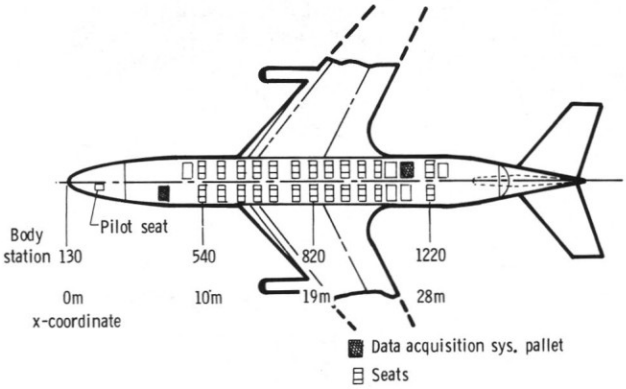

Figure 4. CID Plan View of Aircraft Showing Locations of Seats and Pallets

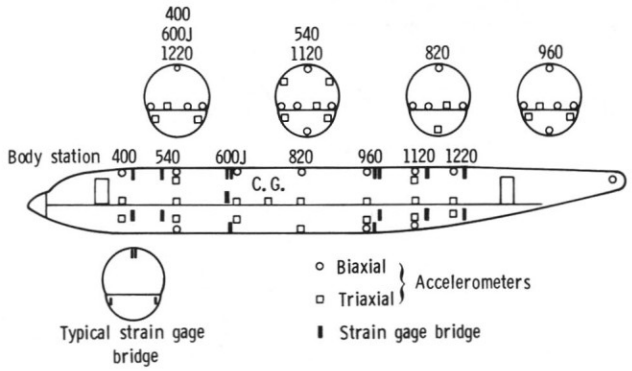

(a) Fuselage

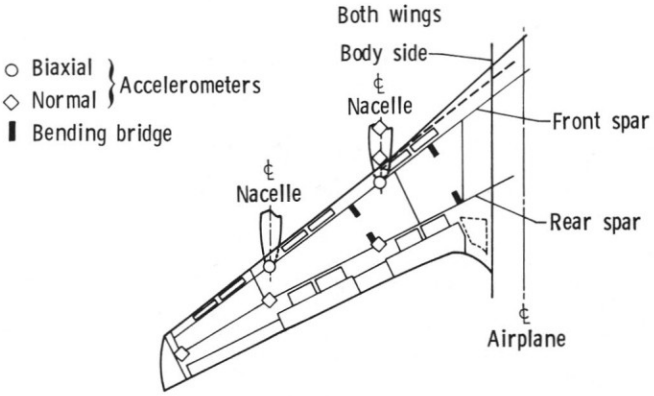

(b) Wing

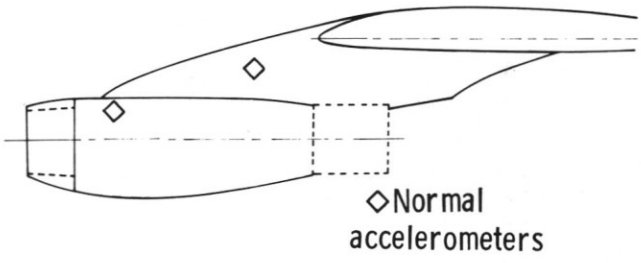

(c) Nacelle

Figure 5. CID Accelerometer and Strain Gage Locations

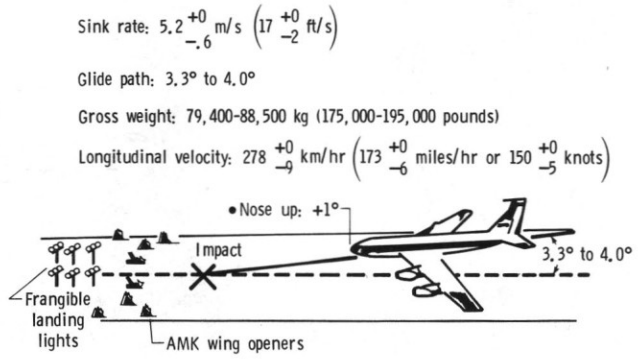

Figure 6. Planned CID Impact Scenario

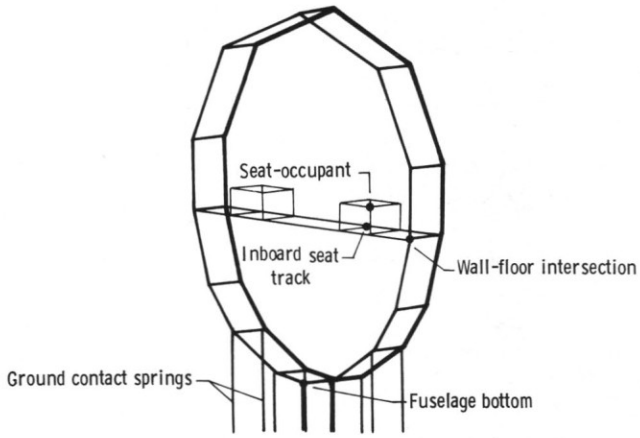

Figure 7. Two-Frame DYCAST Mathematical Model of Fuselage Section

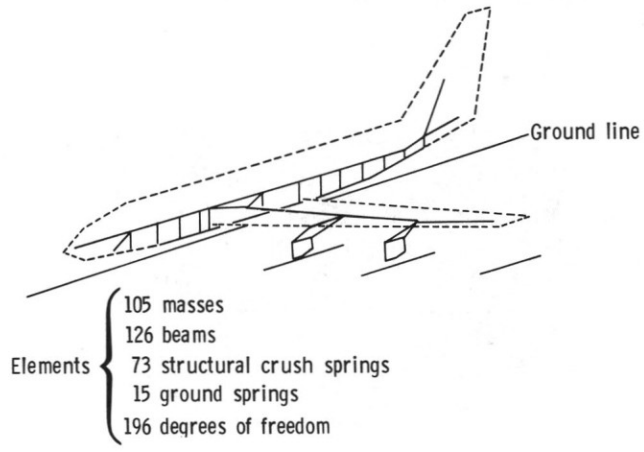

Figure 8. CID DYCAST Symmetric Half-Model

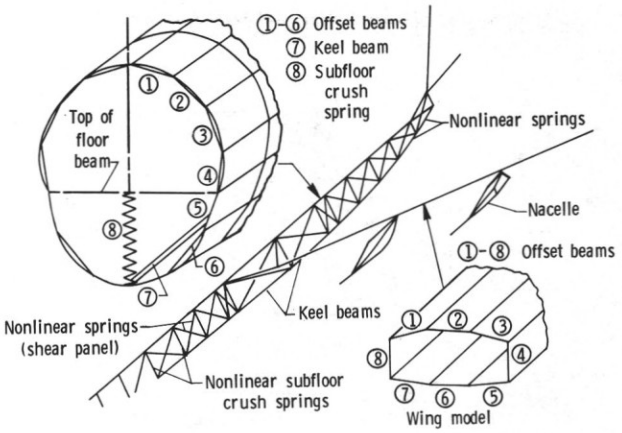

Figure 9. Components of CID DYCAST Model

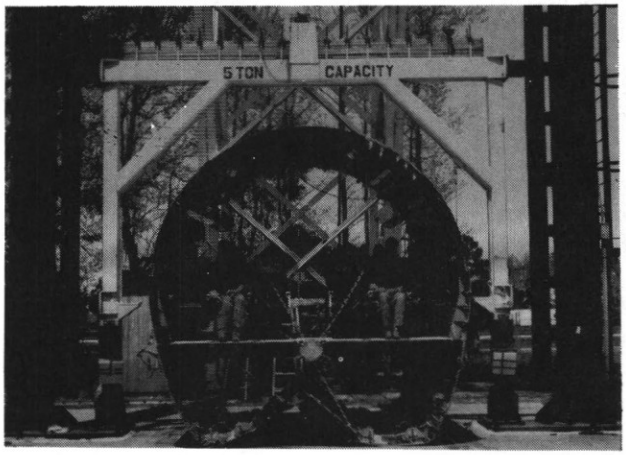

Figure 10. Forward Fuselage Section After Drop Test

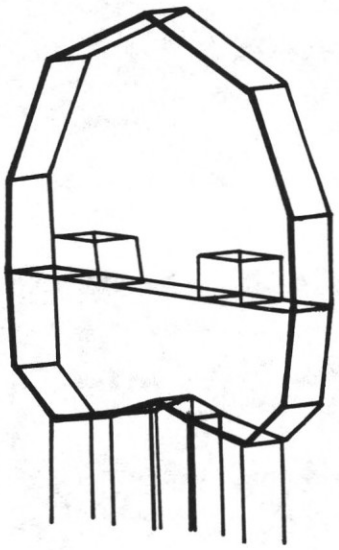

Figure 11. Deformation of Two-Frame DYCAST Model of Forward Fuselage Section

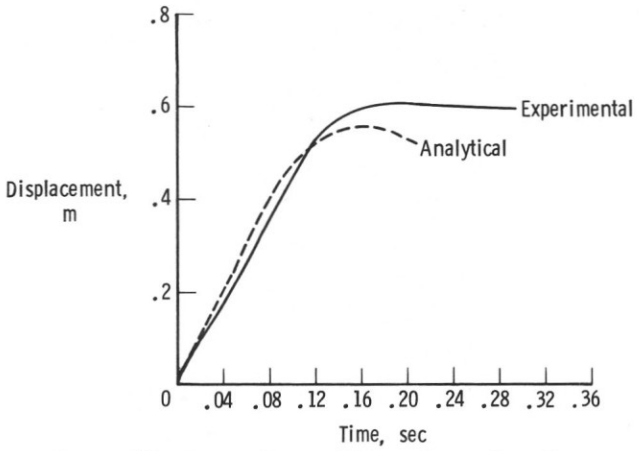

Figure 12. Comparison of Experimental and Analytical Floor Displacements in Forward Fuselage Section Drop Test

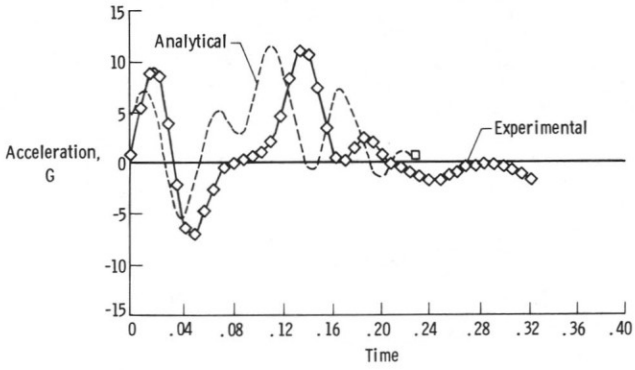

Figure 13. Comparison of Experimental and Analytical Vertical Accelerations at Wall-Floor Interface in Forward Fuselage Section Drop Test

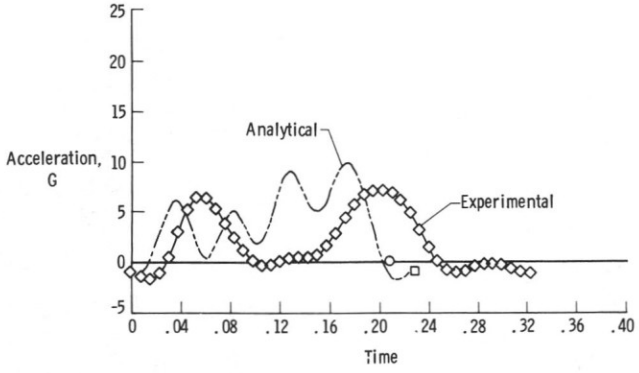

Figure 14. Typical Comparison of Experimental and Analytical Vertical Pelvis Accelerations in Anthropomorphic Dummy in Forward Fuselage Section Drop Test

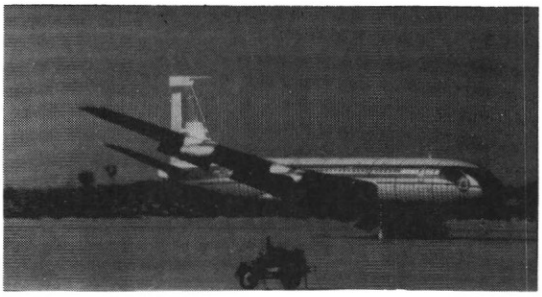

(a) Left wing impact

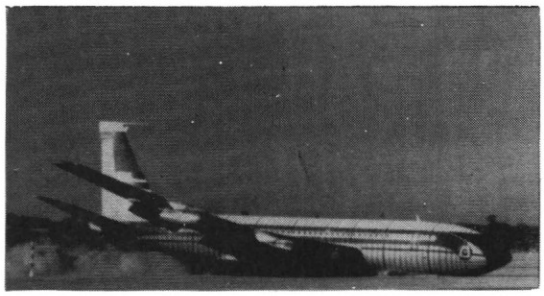

(b) Fuselage impact

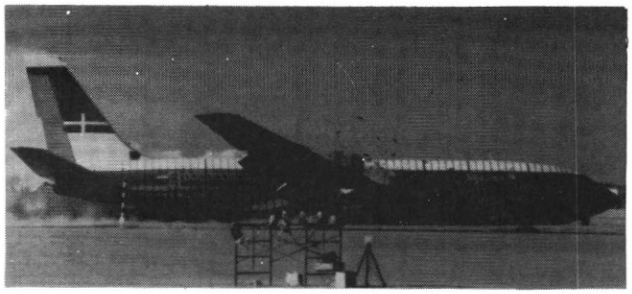

(c) Impact with wing openers

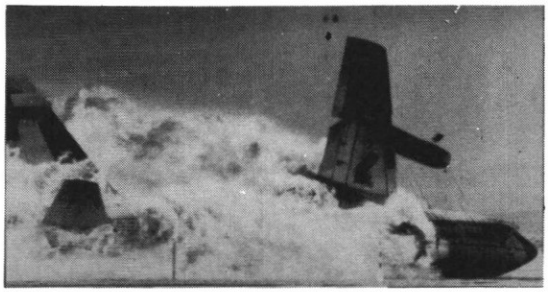

(d) Post crash fire

Figure 15. CID Impact Sequence

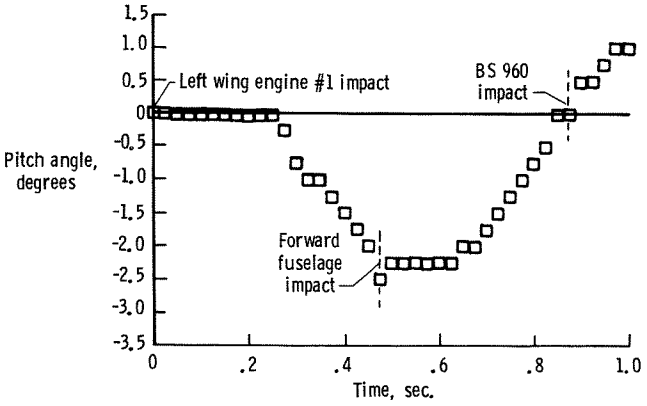

Figure 16. CID Pitch Time History After Initial Left Wing Impact

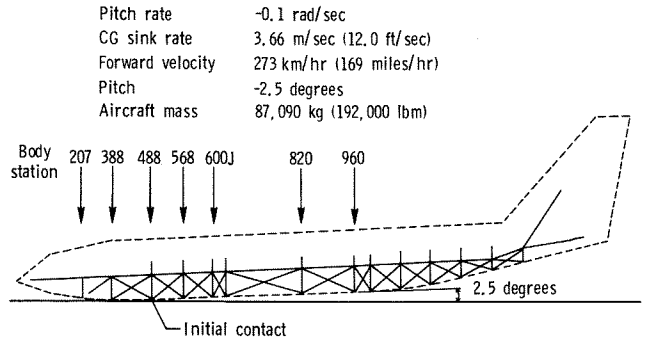

Figure 17. DYCAST Mathematical Model at Fuselage Ground Impact

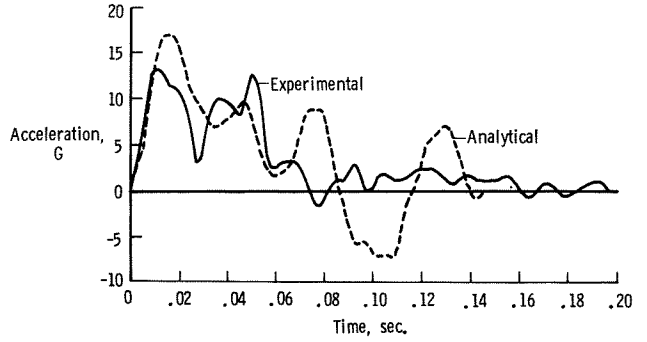

Figure 18. Comparison of Experimental and Analytical Vertical Floor Accelerations at Pilot Location in CID

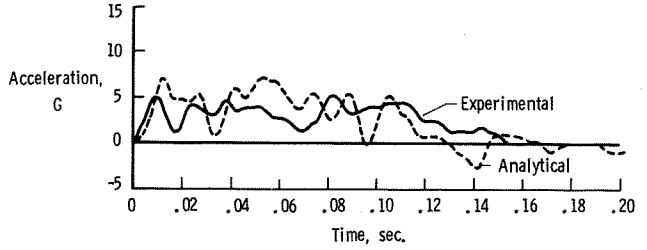

Figure 19. Comparison of Experimental and Analytical Vertical Floor Accelerations at BS 540 in CID

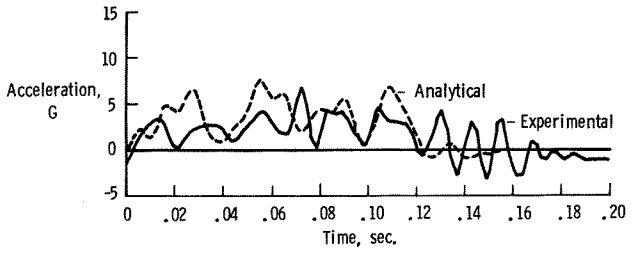

Figure 20. Comparison of Experimental and Analytical Vertical Floor Accelerations at BS 600J in CID

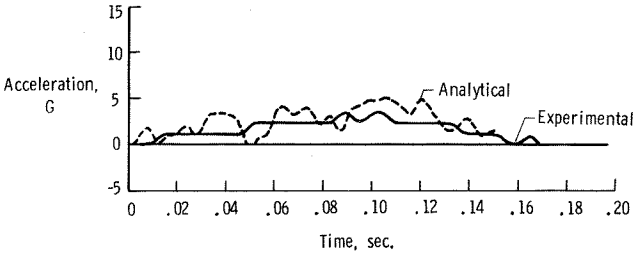

Figure 21. Comparison of Experimental and Analytical Vertical Floor Accelerations at BS 820 in CID

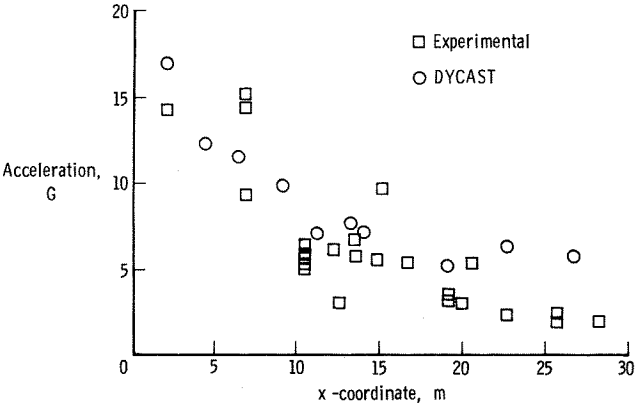

Figure 22. Comparison of Experimental and Analytical Maximum Vertical Floor Accelerations in CID

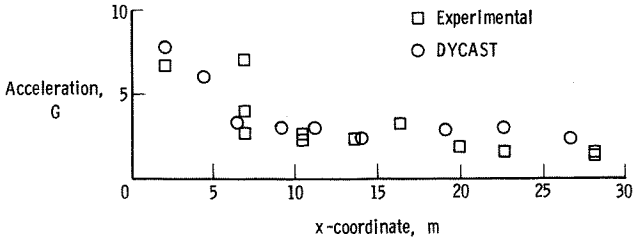

Figure 23. Comparison of Experimental and Analytical Maximum Longitudinal Floor Accelerations in CID

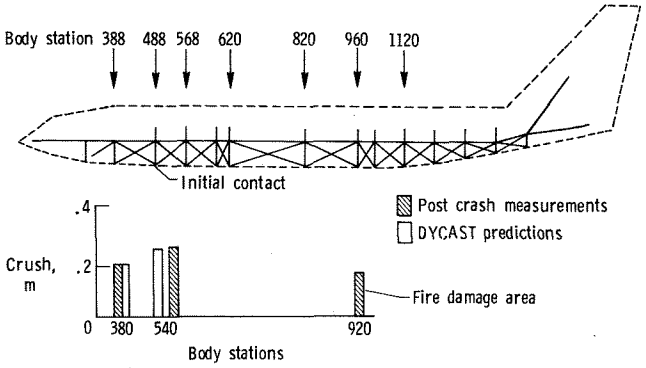

Figure 24. Comparison of Experimental and Analytical Fuselage Crush Displacements in CID